Featured in Physics

Generation of Large Vortex-Free Superfluid Helium Nanodroplets

Anatoli Ulmer,[1,2,*] Andrea Heilrath,[1,3] Björn Senfftleben,[3,4] Sean M. O. O'Connell-Lopez,[5] Björn Kruse,[6] Lennart Seiffert,[6] Katharina Kolatzki,[3,7] Bruno Langbehn,[1] Andreas Hoffmann,[3] Thomas M. Baumann,[4] Rebecca Boll,[4] Adam S. Chatterley,[8] Alberto De Fanis,[4] Benjamin Erk,[9] Swetha Erukala,[5] Alexandra J. Feinberg,[5] Thomas Fennel,[6] Patrik Grychtol,[4] Robert Hartmann,[10] Markus Ilchen,[4,9] Manuel Izquierdo,[4] Bennet Krebs,[6] Markus Kuster,[4] Tommaso Mazza,[4] Jacobo Montaño,[4] Georg Noffz,[1] Daniel E. Rivas,[4] Dieter Schlosser,[10] Fabian Seel,[1] Henrik Stapelfeldt,[8] Lothar Strüder,[10] Josef Tiggesbäumker,[6,11] Hazem Yousef,[4] Michael Zabel,[6] Pawel Ziołkowski,[4] Michael Meyer,[4] Yevheniy Ovcharenko,[4] Andrey F. Vilesov,[5,12] Thomas Möller,[1,†] Daniela Rupp,[3,7,‡] and Rico Mayro P. Tanyag[1,8,§]

[1]*Institute of Optics and Atomic Physics, Technische Universität Berlin, Hardenbergstraße 36, 10623 Berlin, Germany*
[2]*Department of Physics, Universität Hamburg, Luruper Chaussee 149, 22761 Hamburg, Germany*
[3]*Max-Born-Institute for Nonlinear Optics and Short Pulse Spectroscopy, Max-Born-Straße 2A, 12489 Berlin, Germany*
[4]*European XFEL, Holzkoppel 4, 22869 Schenefeld, Germany*
[5]*Department of Chemistry, University of Southern California, 920 Bloom Walk, Los Angeles, California 90089, USA*
[6]*Institute for Physics, Universität Rostock, Albert-Einstein-Straße 23, 18059 Rostock, Germany*
[7]*Laboratory for Solid State Physics, Swiss Federal Institute of Technology in Zurich, John-von-Neumann-Weg 9, 8093 Zurich, Switzerland*
[8]*Department of Chemistry, Aarhus University, Langelandsgade 140, 8000 Aarhus C, Denmark*
[9]*Deutsches Elektronen-Synchrotron DESY, Notkestr. 85, 22607 Hamburg, Germany*
[10]*PNSensor GmbH, Otto-Hahn-Ring 6, 81739 Munich, Germany*
[11]*Department "Life, Light and Matter," Universität Rostock, Albert-Einstein-Straße 23, 18059 Rostock, Germany*
[12]*Department of Physics and Astronomy, University of Southern California, 920 Bloom Walk, Los Angeles, California 90089, USA*

(Received 14 February 2023; accepted 22 June 2023; published 16 August 2023)

Superfluid helium nanodroplets are an ideal environment for the formation of metastable, self-organized dopant nanostructures. However, the presence of vortices often hinders their formation. Here, we demonstrate the generation of vortex-free helium nanodroplets and explore the size range in which they can be produced. From x-ray diffraction images of xenon-doped droplets, we identify that single compact structures, assigned to vortex-free aggregation, prevail up to 10^8 atoms per droplet. This finding builds the basis for exploring the assembly of far-from-equilibrium nanostructures at low temperatures.

DOI: 10.1103/PhysRevLett.131.076002

The visualization of dopant nanostructures formed inside a helium droplet offers an opportunity to parse the factors driving their self-assembly in a cold, superfluid environment, including the effect of intermolecular forces among the dopant materials and their attraction to quantized vortices, if present. While helium nanodroplets have long been used as a matrix for cooling and preparing dopants for their spectroscopic studies [1,2], it is only through x-ray coherent diffractive imaging that the visualization of both the droplets and dopant nanostructures has become possible [3,4]. One testament to this imaging technology is the captured *in situ* configurations of xenon-traced vortex filaments in submicron-sized superfluid helium droplets [5–10].

Vortices with quantized circulation are a manifestation of superfluidity and play an essential role in the rotational dynamics of both Bose–Einstein condensates and superfluid helium [11–14]. Although these vortices are fascinating and intriguing by themselves, their presence dominates nanostructure formation since many dopants are easily attracted to them [9,10,15–18]. On the other hand, in their absence, the dopants may be randomly distributed inside the confined droplet space because of the droplet's superfluid state and the weak interaction between helium and the dopant [1,2,19,20]. Additionally, since any heat associated with the doping process and dopant aggregation are rapidly dissipated through the evaporation of helium atoms, the dopants could form amorphous particles with a fractallike substructure influenced by intermolecular forces [19,21–24]. In small helium nanodroplets containing

a few tens of thousands of atoms, examples of spectroscopically identified nanostructures include silver forming compact clusters at one or several sites in the droplet [20]; hydrogen cyanide assembling into linear chains [25]; water forming the smallest observed ice nanostructure with only six molecules [21]; weakly bound magnesium aggregating in a foam structure [26,27]; and a core-shell structure of a multicomponent doped droplet [28–30].

To explore and image self-organized structures, especially those that can only be formed in superfluid droplets, the presence of vortices needs to be suppressed. One means of controlling their presence is to generate the droplets by expanding cold helium gas. Here, nanodroplets may be stochastically formed from the initial condensation of helium into small clusters that further grow through collision with other helium clusters at some distance away from the nozzle [31]. This way of droplet generation may preclude the acquisition of angular momentum from shear forces prompted by the coflowing helium fluid. In this Letter, we demonstrate that droplets produced from gas condensation using a conical nozzle are larger and have smaller rotational distortion as compared to those produced using a pinhole nozzle in previous experiments [5,8,32,33]. Smaller shape deformations indicate a smaller angular momentum of the droplets, which likely contain few if any vortices. Because of this effect, we could identify two major types of xenon nanostructures, filaments and compact, that are respectively assigned to vortex-induced [6–10,34–36], and vortex-free aggregation. Finally, we map the occurrence of these two structures based on the droplet size and find that droplets smaller than ∼200 nm in diameter are conducive to imaging far-from-equilibrium nanostructures; opening routes for studying self-assembly in a self-bound superfluid droplet.

X-ray coherent diffractive imaging was performed at the Nano-sized Quantum Systems end station of the European XFEL's Small Quantum Systems scientific instrument [37,38]. This imaging technique takes snapshots of the droplet size and shape and, if doped, the structure of the dopant aggregates [3,4]. The helium droplets were produced using a conical nozzle with a throat diameter of 150 μm, a half-opening angle of 3°, and a channel length of 9.3 mm. The nozzle was attached to a Parker valve and operated at a constant stagnation pressure of 20 bar, while the nozzle temperature T_0 was varied from 5 K to 14 K. Variable amounts of xenon were introduced in a gas doping cell installed along the droplet's flight path. At ∼1.05 meters from the nozzle exit, the droplets reached the interaction volume where they intersected the x-ray beam that had a photon energy of 1 keV, pulse energies in the range of 3 mJ to 5 mJ, and a focus diameter of ∼1.5 μm (FWHM) [38]. The scattered light from a diffraction event was collected up to 6° by an area detector located ∼370 mm from the interaction volume [37]. A detailed description of the experiment and other relevant information are given in the Supplemental Material (SM) [39].

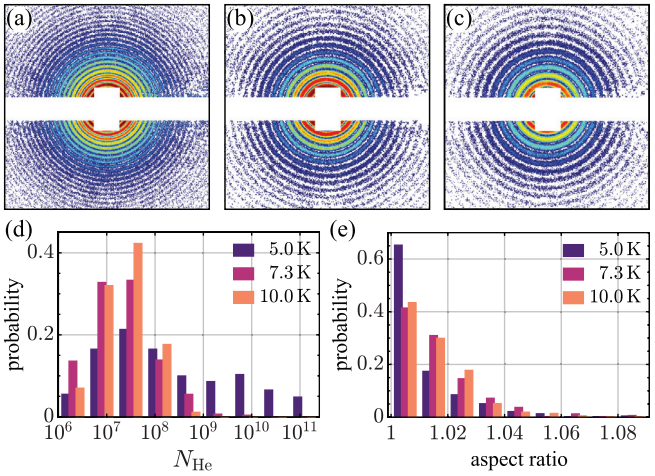

FIG. 1. Selected diffraction images of pure droplets obtained at a nozzle temperature of (a) 5.0 K, (b) 7.3 K, and (c) 10.0 K. The size distributions are given in panel (d), and their aspect ratio distributions in panel (e). The numbers of diffraction images used for the size (aspect ratio) distributions are 291 (236) for 5.0 K, 766 (488) for 7.3 K, and 272 (214) for 10.0 K.

Figures 1(a)–1(c) show examples of diffraction images for pure (i.e., undoped) droplets produced at $T_0 = 5.0$ K, 7.3 K, and 10.0 K, respectively. The size distributions are depicted in Fig. 1(d) where the droplet size N_{He} is customarily given as the number of helium atoms and is related to the droplet's radius R_{D} through $N_{\mathrm{He}} = (R_{\mathrm{D}}/0.222\ \mathrm{nm})^3$ [1,2]. The nozzle temperatures explored here encompass two droplet production regimes: the fragmentation of liquid helium close to the nozzle throat at $T_0 = 5$ K, and the condensation of helium gas after the nozzle throat at $T_0 \geq 10$ K [1,2]. The size distribution at $T_0 = 5$ K is bimodal with a broad size range, whereas, that for $T_0 \geq 10$ K is more narrow with an almost log-normal shape. Under similar stagnation conditions, the droplets produced at the gas condensation regime using the conical nozzle are about two to three orders of magnitude larger than those produced using the 5 μm pinhole nozzle [1,2], also see Fig. S7 in the SM [39].

As with rotating viscous liquid drops [81], a rotating superfluid helium droplet can have a series of equilibrium shapes depending on its angular velocity and angular momentum [82,83]. One way to describe a droplet's shape is through its aspect ratio AR, which is defined as the ratio between the semimajor and semiminor axes of the projected droplet density onto a two-dimensional plane. Figure 1(e) shows the aspect ratio distribution for $T_0 = 5.0$ K, 7.3 K, and 10.0 K with average values of $(1.011^{+0.012}_{-0.011})$, (1.016 ± 0.013), and (1.015 ± 0.012), respectively. Collectively, 96.4% (99.9%) of the droplets generated using the conical nozzle have an aspect ratio smaller than 1.05 (1.10), making them close to spherical,

and the largest observed AR is 1.3. These values are considerably smaller than those obtained from previous investigations using different kinds of nozzles. For instance, values as high as 2.3 have been reported for droplets produced from a 5 μm pinhole nozzle at 20 bar and 5 K with ∼65% of the droplets having $AR \leq 1.05$ [84]. Another experiment using a flow cryostat but with the same 5 μm pinhole nozzle at $T_0 \simeq 5$ K reported a mean value $\langle AR \rangle = 1.059 \pm 0.005$, with 1% of the droplets exhibiting $AR \geq 1.4$ [33]. For droplets produced at 80 bar and 5.4 K using a trumpet-shaped nozzle with a throat diameter of 100 μm and a half-opening angle of 20°, aspect ratios as large as ∼3 were observed, and 92.9% of the droplets have close-to-spherical shape [85]. Further elaboration about the droplets produced using these three nozzles is included in the SM [39].

The consequence of generating close-to-spherical and large superfluid nanodroplets is reflected on the types of nanostructures observed inside them. Figure 2 shows

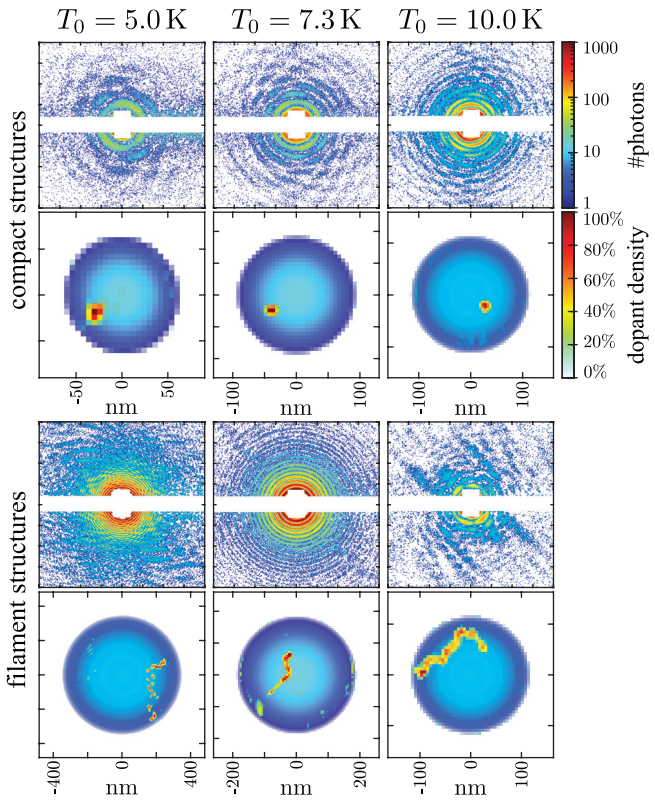

FIG. 2. Major types of xenon nanostructures inside helium droplets generated using a conical nozzle at different nozzle temperatures T_0. Shown are selected examples of compact structures from vortex-free droplets and filaments from vortex-hosting ones. For each structure type, the first row shows the measured diffraction image, whereas the second shows the numerically reconstructed xenon-doped droplets using a modified DCDI, see the SM [39]. The nm scale is different in each figure. The droplet is shown in blue colors, while the droplet density scales with the brightness. The color scales for the diffraction and the dopant reconstruction are shown on the upper right portion.

diffraction images and numerically reconstructed xenon clusters in droplets generated at different nozzle temperatures. The image reconstruction algorithm is a modified version of the droplet coherent diffractive imaging (DCDI) [6,39]. In each reconstruction, the droplet is represented by dark blue to blue colors, while the xenon clusters are represented by dark red to light green colors. Two major kinds of structures were observed: compact (upper panel) and filaments (lower panel). The compact structures are assigned to vortex-free aggregation, are located at some distance away from the droplet's center, and have roughly circular shapes with radii ranging from 10 nm to 15 nm. Because of the high thermal conductivity of superfluid helium, these compact structures possibly grow with an amorphous or even fractal morphology as similarly observed in bulk superfluid helium [23,24,86]. Compact structures larger than 20 nm are also observed (see Fig. S5 in SM [39]), but instead of having a more circular shape, they seem to be composed of two clusters, where each may have initially been formed at different aggregation sites before colliding and fusing into a cluster-cluster aggregate. However, because the heat of condensation is not enough to melt them, the two clusters remain distinct without reforming into one big clump [23].

Similar to previous observations [5–10], the filaments are also assigned to xenon clusters tracing the vortex length. In contrast, however, the number of vortices in our experiment is rather few (< 6), and no Bragg peaks, whose occurrence in a diffraction attests to the presence of a vortex lattice [5,8], were observed. The off-centered single vortices in Fig. 2 convey that the xenon distribution along the vortex line is uneven; rather, each is dotted by distinct nanometer-sized (10 to 20 nm) xenon clusters. Additionally, the filament is not smooth and its curvature is not as expected for an off-centered vortex [15,87]. Instead, it has oscillations along its length that specify underlying dynamics of how dopants approach a vortex [16,17,86,88] and indicate the presence of helical Kelvin waves relevant to quantum turbulence and the cascade of excitations in superfluids [11,89,90]. This observation of single vortices is instrumental to understanding vortex nucleation and decay in a superfluid helium droplet, as similarly observed in Bose–Einstein condensates [91,92].

Crucial to distinguishing these two nanostructures is the droplet's angular momentum, which may be partitioned between quantum vortices and capillary waves. Almost all droplets in earlier imaging experiments were generated in the liquid fragmentation regime and contained multiple vortices [5–10,32,33,85,93]. These droplets probably acquire angular momentum through the shear flow of the expanding helium fluid [32–34]. A smaller nozzle orifice, or higher velocities due to higher stagnation pressures of the expanding fluid, increases the action of shear forces that translates to a larger vorticity of the fluid flow. Within a few nanoseconds during flight, the droplets

become superfluid via evaporative cooling and reach a temperature of ∼0.4 K after ∼100 μs [18] with the angular momentum conserved. If the acquired angular momentum is sufficient, one or more stable quantized vortices are nucleated. If more than enough is acquired, multiple vortices form a triangular lattice with the same quantum of circulation and sense of rotation [11,14] and bear most of the droplet's angular momentum [8,82,83]. At high angular momentum, the velocity fields from the vortices and the capillary waves induce deformations that resemble the equilibrium shapes of rotating classical viscous droplets [8,82,83], i.e., from spherical to oblate and to triaxial prolate shapes at higher angular momenta [5,8,32,33,85]. The angular momentum required for a single straight vortex to reside in the droplet's center is equal to $N_{\mathrm{He}}\hbar$ [15,82,83,87,94]. If less angular momentum is present, an off-axis curved vortex may be created that precesses around the droplet's center and whose angular momentum decreases with its curvature [15,16,87]. On the other hand, if the acquired angular momentum is insufficient for vortex nucleation, it may be stored as capillary waves, and, in this case, the droplets can only rotate by adopting prolate-shape configurations [82,83,94]. In the present experiment, the close-to-spherical droplets suggest that they contain small angular momenta, consistent with the observation of the absence or a small number of vortices, see the SM for further discussion [39]. However, the exact partition of the small angular momenta between few vortices and capillary waves requires further theoretical and experimental studies, especially for submicron to millimeter-sized superfluid drops [95].

The finding that compact structures are mainly observed in smaller droplets and filaments in larger ones can be used to locate the droplet sizes where the formation of either structure is favored. Figure 3 shows the abundance and fractions of these xenon structures for $T_0 = 5$ K (top), 7.3 K (middle), and 10 K (bottom). The vertical dashed lines on the fraction panel indicate that the transition crossover, or where the onset of vortex-induced xenon aggregation is facilitated, occurs at $N_{\mathrm{He}} \approx 10^8$, almost independent of how the droplets are generated. Nevertheless, the means of droplet generation affects the relative abundance of either structures. For instance, filaments are dominant in the liquid fragmentation regime at $T_0 = 5$ K, and conversely, compact structures in the gas condensation regime at $T_0 \geq 10$ K. The observation of filaments in the gas condensation regime is interesting since it suggests that angular momentum was acquired during droplet growth, possibly from droplet collision. A simple kinematic model to estimate the acquired angular momentum shows that for the same collision velocity the angular momentum per atom increases with droplet size, and plausibly why smaller droplets are vortex free [39]. In other words, larger droplets require slower collision velocities to have the same angular momentum per atom as compared to smaller droplets. Moreover, these larger droplets also need less angular momentum per atom to maintain a stable curved

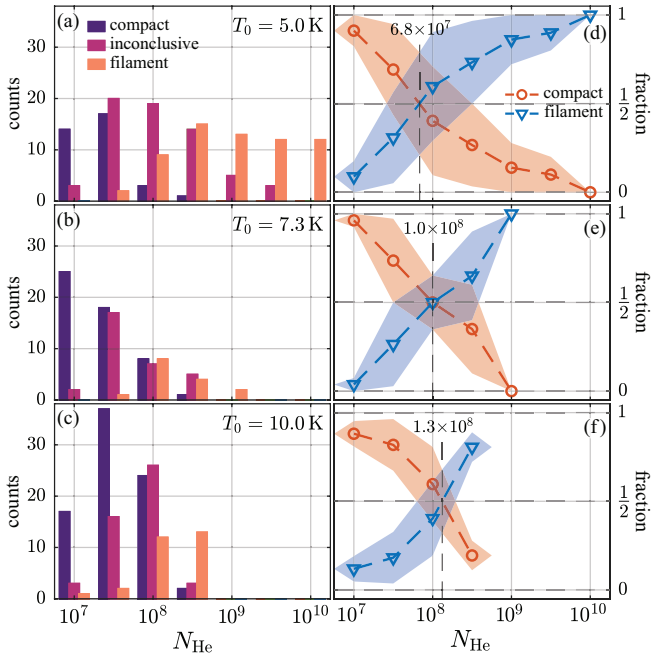

FIG. 3. Mapping structure formation as a function of the droplet size. The counts (a)–(c) and fractions (d)–(f) of the identified compact and filament xenon nanostructures for $T_0 = 5$ K, 7.3 K, and 10 K (from top to bottom). Structures that could not be assigned to either categories are categorized as inconclusive (see Fig. S5 in SM [39]) and serve as identification error for the fraction diagrams.

vortex [15,39]. These estimates corroborate the observed size-dependent vortex stability in superfluid helium droplets. Finally, at 12 K and 20 bar, only compact structures were found, but both structures with a similar crossover were observed again when the stagnation pressure was increased to 60 bar, see Fig. S8 in SM [39].

In summary, we have demonstrated that large superfluid helium nanodroplets generated using a large-diameter conical nozzle are close to spherical where the angular momentum is likely shared between a few vortices and surface capillary waves. Additionally, we distinguished two main types of dopant aggregation, where their relative abundance is droplet size dependent. The size-dependent transition from vortex-free to vortex-induced structures also emphasizes the size dependence of the rotational state of superfluid helium droplets. For instance, xenon-traced vortex filaments are only readily observed in droplets with more than 10^8 helium atoms. This size not only benchmarks the onset where vortex-induced nanostructure formation starts to be dominant, but it also indicates the droplet size amenable for the preparation of self-organized nanostructures without the influence of quantum vortices. This study could be a beginning for x-ray imaging of far-from-equilibrium nanostructures from various kinds of dopant materials with different intermolecular forces (e.g., hydrogen or metallic bonding). Without the influence of vortices, it also becomes possible to image dynamics (e.g., nanosplasma ignition)

occurring between the dopants and the droplet (in contrast to the observation in Ref. [96]), and how charges are distributed on the droplet's surface [10].

Data recorded for the experiment at the European XFEL are available at [97].

We acknowledge the European XFEL in Schenefeld, Germany for the beamtime allocation (SQS 2195) at the SQS instrument, and for the user financial support grant. We would also like to thank the staff, especially Steffen Hauf, for their enormous assistance. We thank the precision mechanics workshops at the TU Berlin Physics Department and Max-Born-Institut for their technical support. Additionally, we greatly benefited from discussions about droplet collisions, nucleation of vortices, and rotation of prolate-shaped droplets from Manuel Barranco, Francesco Ancilotto, and Martí Pi. A. U., R. M. P. T., D. R., T. Mö., J. T., Be. K., and M. Z. acknowledge funding provided by the Bundesministerium für Bildung und Forschung (BMBF) via Grant No. 05K16KT3, the BMBF Forschungs schwerpunkt Freie-Elektronen-Laser FSP-302, Deutsche Forschungsgemeinschaft (DFG) Mo 719/13 and Mo 719/14. A. U. and M. M. acknowledge support by the Cluster of Excellence "Advanced Imaging of Matter" of the DFG—EXC 2056—project 390715994. Additionally, M. M. acknowledges support by the DFG—SFB-925—project 170620586. A. H., B. S., K. K., A. H., and D. R. acknowledge funding from the Leibniz-Gemeinschaft via Grant No. SAW/2017/MBI4, and K. K. and D. R. further acknowledge the Swiss National Science Foundation under the Grant No. 200021E_193642. S. M. O. O-L., S. E., A. J. F., and A. F. V. were supported by the National Science Foundation (NSF) under Grants No. CHE-1664990 and No. CHE-2102318, and by NSF Grants No. DMR-1701077 and No. DMR-2205081. H. S. and R. M. P. T acknowledge support from Villum Fonden through a Villum Investigator Grant No. 25886. T. F. and J. T. acknowledge support by the DFG via SFB 1477 "light-matter interactions at interfaces" (ID: 441234705). T. F. further acknowledge support by the Heisenberg program (ID: 436382461). J. T. further acknowledge support by the DFG via TI 210/13-1. M. I. acknowledges funding from the Volkswagen Foundation for a Peter-Paul-Ewald Fellowship. Bj. K. gratefully acknowledges funding by the European Social Fund (ESF) and the Ministry of Education, Science and Culture of Mecklenburg-Western Pomerania (Germany) within the project NEISS (Neural Extraction of Information, Structure and Symmetry in Images) under Grant No. ESF/14-BM-A55-0007/19.

[*]Corresponding author.
anatoli.ulmer@physik.tu-berlin.de
[†]Corresponding author.
thomas.moeller@physik.tu-berlin.de
[‡]Corresponding author.
ruppda@phys.ethz.ch
[§]Corresponding author.
tanyag@physik.tu-berlin.de

[1] J. P. Toennies and A. F. Vilesov, Superfluid helium droplets: A uniquely cold nanomatrix for molecules and molecular complexes, Angew. Chem. Int. Ed. **43**, 2622 (2004).
[2] *Molecules in Superfluid Helium Nanodroplets: Spectroscopy, Structure, and Dynamics*, edited by A. Slenczka and J. P. Toennies, Topics in Applied Physics Vol. 145 (Springer International Publishing, Cham, 2022).
[3] O. Gessner and A. F. Vilesov, Imaging quantum vortices in superfluid helium droplets, Annu. Rev. Phys. Chem. **70**, 173 (2019).
[4] R. M. P. Tanyag, B. Langbehn, T. Möller, and D. Rupp, X-ray and XUV imaging of helium nanodroplets, in *Molecules in Superfluid Helium Nanodroplets: Spectroscopy, Structure, and Dynamics*, edited by A. Slenczka and J. P. Toennies (Springer International Publishing, Cham, 2022), pp. 281–341.
[5] L. F. Gomez *et al.*, Shapes and vorticities of superfluid helium nanodroplets, Science **345**, 906 (2014).
[6] R. M. P. Tanyag *et al.*, Communication: X-ray coherent diffractive imaging by immersion in nanodroplets, Struct. Dyn. **2**, 051102 (2015).
[7] C. F. Jones *et al.*, Coupled motion of Xe clusters and quantum vortices in He nanodroplets, Phys. Rev. B **93**, 180510(R) (2016).
[8] S. M. O. O'Connell, R. M. P. Tanyag, D. Verma, C. Bernando, W. Pang, C. Bacellar, C. A. Saladrigas, J. Mahl, B. W. Toulson, Y. Kumagai, P. Walter, F. Ancilotto, M. Barranco, M. Pi, C. Bostedt, O. Gessner, and A. F. Vilesov, Angular Momentum in Rotating Superfluid Droplets, Phys. Rev. Lett. **124**, 215301 (2020).
[9] A. J. Feinberg, D. Verma, S. M. O'Connell-Lopez, S. Erukala, R. M. P. Tanyag, W. Pang, C. A. Saladrigas, B. W. Toulson, M. Borgwardt, N. Shivaram, M.-F. Lin, A. A. Haddad, W. Jäger, C. Bostedt, P. Walter, O. Gessner, and A. F. Vilesov, Aggregation of solutes in bosonic versus fermionic quantum fluids, Sci. Adv. **7**, eabk2247 (2021).
[10] A. J. Feinberg *et al.*, X-ray diffractive imaging of highly ionized helium nanodroplets, Phys. Rev. Res. **4**, L022063 (2022).
[11] R. J. Donnelly, *Quantized Vortices in Helium II*, Cambridge Studies in Low Temperature Physics Vol. 3 (Cambridge University Press, Cambridge, UK, 1991).
[12] F. Dalfovo and S. Stringari, Helium nanodroplets and trapped Bose–Einstein condensates as prototypes of finite quantum fluids, J. Chem. Phys. **115**, 10078 (2001).
[13] A. L. Fetter, Rotating trapped Bose–Einstein condensates, Rev. Mod. Phys. **81**, 647 (2009).
[14] C. Barenghi and N. G. Parker, *A Primer on Quantum Fluids*, SpringerBriefs in Physics (Springer International Publishing, Cham, 2016).
[15] K. K. Lehmann and R. Schmied, Energetics and possible formation and decay mechanisms of vortices in helium nanodroplets, Phys. Rev. B **68**, 224520 (2003).
[16] F. Coppens, F. Ancilotto, M. Barranco, N. Halberstadt, and M. Pi, Capture of Xe and Ar atoms by quantized vortices in

^{4}He nanodroplets, Phys. Chem. Chem. Phys. **19**, 24805 (2017).
[17] F. Coppens, F. Ancilotto, M. Barranco, N. Halberstadt, and M. Pi, Dynamics of impurity clustering in superfluid ^{4}He nanodroplets, Phys. Chem. Chem. Phys. **21**, 17423 (2019).
[18] R. M. P. Tanyag, C. F. Jones, C. Bernando, S. M. O. O'Connell, D. Verma, and A. F. Vilesov, CHAPTER 8 Experiments with Large Superfluid Helium Nanodroplets, in *Cold Chemistry: Molecular Scattering and Reactivity Near Absolute Zero*, edited by O. Dulieu and A. Osterwalder (The Royal Society of Chemistry, London, 2018), pp. 389–443.
[19] M. Lewerenz, B. Schilling, and J. P. Toennies, Successive capture and coagulation of atoms and molecules to small clusters in large liquid helium clusters, J. Chem. Phys. **102**, 8191 (1995).
[20] E. Loginov, L. F. Gomez, N. Chiang, A. Halder, N. Guggemos, V. V. Kresin, and A. F. Vilesov, Photoabsorption of $Ag_N(N \sim 6$–$6000)$ Nanoclusters Formed in Helium Droplets: Transition from Compact to Multicenter Aggregation, Phys. Rev. Lett. **106**, 233401 (2011).
[21] K. Nauta and R. E. Miller, Formation of cyclic water hexamer in liquid helium: The smallest piece of ice, Science **287**, 293 (2000).
[22] S. G. Alves, A. F. Vilesov, and S. C. Ferreira, Effects of the mean free path and relaxation in a model for the aggregation of particles in superfluid media, J. Chem. Phys. **130**, 244506 (2009).
[23] E. B. Gordon, The influence of superfluidity on impurities condensation in liquid helium, Low Temp. Phys. **38**, 1043 (2012).
[24] R. E. Boltnev, I. B. Bykhalo, and I. N. Krushinskaya, Impurity systems in condensed helium-4, J. Low Temp. Phys. **208**, 50 (2022).
[25] K. Nauta and R. E. Miller, Nonequilibrium self-assembly of long chains of polar molecules in superfluid helium, Science **283**, 1895 (1999).
[26] A. Przystawik, S. Göde, T. Döppner, J. Tiggesbäumker, and K.-H. Meiwes-Broer, Light-induced collapse of metastable magnesium complexes formed in helium nanodroplets, Phys. Rev. A **78**, 021202(R) (2008).
[27] S. Göde, R. Irsig, J. Tiggesbäumker, and K.-H. Meiwes-Broer, Time-resolved studies on the collapse of magnesium atom foam in helium nanodroplets, New J. Phys. **15**, 015026 (2013).
[28] E. Loginov, L. F. Gomez, and A. F. Vilesov, Formation of core–shell silver–ethane clusters in He droplets, J. Phys. Chem. A **117**, 11774 (2013).
[29] E. Loginov, L. F. Gomez, B. G. Sartakov, and A. F. Vilesov, Formation of core–shell ethane–silver clusters in He droplets, J. Phys. Chem. A **121**, 5978 (2017).
[30] G. Haberfehlner, P. Thaler, D. Knez, A. Volk, F. Hofer, W. E. Ernst, and G. Kothleitner, Formation of bimetallic clusters in superfluid helium nanodroplets analysed by atomic resolution electron tomography, Nat. Commun. **6**, 8779 (2015).
[31] M. A. Ratner, Kinetics of cluster growth in expanding rare-gas jet, Low Temp. Phys. **25**, 266 (1999).
[32] C. Bernando *et al.*, Shapes of rotating superfluid helium nanodroplets, Phys. Rev. B **95**, 064510 (2017).
[33] D. Verma, S. M. O. O'Connell, A. J. Feinberg, S. Erukala, R. M. P. Tanyag, C. Bernando, W. Pang, C. A. Saladrigas, B. W. Toulson, M. Borgwardt, N. Shivaram, M.-F. Lin, A. Al Haddad, W. Jäger, C. Bostedt, P. Walter, O. Gessner, and A. F. Vilesov, Shapes of rotating normal fluid ^{3}He versus superfluid ^{4}He droplets in molecular beams, Phys. Rev. B **102**, 014504 (2020).
[34] L. F. Gomez, E. Loginov, and A. F. Vilesov, Traces of Vortices in Superfluid Helium Droplets, Phys. Rev. Lett. **108**, 155302 (2012).
[35] E. Latimer, D. Spence, C. Feng, A. Boatwright, A. M. Ellis, and S. Yang, Preparation of ultrathin nanowires using superfluid helium droplets, Nano Lett. **14**, 2902 (2014).
[36] A. Volk, P. Thaler, D. Knez, A. W. Hauser, J. Steurer, W. Grogger, F. Hofer, and W. E. Ernst, The impact of doping rates on the morphologies of silver and gold nanowires grown in helium nanodroplets, Phys. Chem. Chem. Phys. **18**, 1451 (2016).
[37] M. Kuster *et al.*, The 1-megapixel pnCCD detector for the small quantum systems instrument at the European XFEL: System and operation aspects, J. Synchrotron Radiat. **28**, 576 (2021).
[38] T. Mazza *et al.*, The beam transport system for the small quantum systems instrument at the European XFEL: Optical layout and first commissioning results, J. Synchrotron Radiat. **30**, 457 (2023).
[39] See Supplemental Material at http://link.aps.org/supplemental/10.1103/PhysRevLett.131.076002, which includes Refs. [40–80], and details on the experimental setup, image data processing, estimation of the droplet's angular momenta, and a description and comparison of the different kinds of nozzles used in generating helium droplets.
[40] O. F. Hagena and W. Obert, Cluster formation in expanding supersonic jets: Effect of pressure, temperature, nozzle size, and test gas, J. Chem. Phys. **56**, 1793 (1972).
[41] O. F. Hagena, Nucleation and growth of clusters in expanding nozzle flows, Surf. Sci. **106**, 101 (1981).
[42] E. L. Knuth, Size correlations for condensation clusters produced in free-jet expansions, J. Chem. Phys. **107**, 9125 (1997).
[43] L. F. Gomez, E. Loginov, R. Sliter, and A. F. Vilesov, Sizes of large He droplets, J. Chem. Phys. **135**, 154201 (2011).
[44] H. C. Hulst, *Light Scattering by Small Particles* (Dover Publications, Inc., New York, 1981).
[45] D. Starodub, P. Rez, G. Hembree, M. Howells, D. Shapiro, H. N. Chapman, P. Fromme, K. Schmidt, U. Weierstall, R. B. Doak, and J. C. H. Spence, Dose, exposure time and resolution in serial x-ray crystallography, J. Synchrotron Radiat. **15**, 62 (2008).
[46] A. Rose, *Television Pickup Tubes and the Problem of Vision* (Academic Press, New York, 1948), pp. 131–166.
[47] H. N. Chapman, A. Barty, S. Marchesini, A. Noy, S. P. Hau-Riege, C. Cui, M. R. Howells, R. Rosen, H. He, J. C. H. Spence, U. Weierstall, T. Beetz, C. Jacobsen, and D. Shapiro, High-resolution *ab initio* three-dimensional x-ray diffraction microscopy, J. Opt. Soc. Am. A **23**, 1179 (2006).

[48] A. Schropp and C. G. Schroer, Dose requirements for resolving a given feature in an object by coherent x-ray diffraction imaging, New J. Phys. **12**, 035016 (2010).
[49] A. V. Martin *et al.*, Noise-robust coherent diffractive imaging with a single diffraction pattern, Opt. Express **20**, 16650 (2012).
[50] R. J. Donnelly and C. F. Barenghi, The observed properties of liquid helium at the saturated vapor pressure, J. Phys. Chem. Ref. Data **27**, 1217 (1998).
[51] J. M. Escartín, F. Ancilotto, M. Barranco, and M. Pi, Merging of superfluid helium nanodroplets with vortices, Phys. Rev. B **105**, 024511 (2022).
[52] H. Buchenau, E. L. Knuth, J. Northby, J. P. Toennies, and C. Winkler, Mass spectra and time of flight distributions of helium cluster beams, J. Chem. Phys. **92**, 6875 (1990).
[53] J. Harms, J. P. Toennies, and E. L. Knuth, Droplets formed in helium free-jet expansions from states near the critical point, J. Chem. Phys. **106**, 3348 (1997).
[54] J. P. Toennies and K. Winkelmann, Theoretical studies of highly expanded free jets: Influence of quantum effects and a realistic intermolecular potential, J. Chem. Phys. **66**, 3965 (1977).
[55] J. M. Soler, N. García, O. Echt, K. Sattler, and E. Recknagel, Microcluster Growth: Transition from Successive Monomer Addition to Coagulation, Phys. Rev. Lett. **49**, 1857 (1982).
[56] D. Rupp, M. Adolph, T. Gorkhover, S. Schorb, D. Wolter, R. Hartmann, N. Kimmel, C. Reich, T. Feigl, A. R. B. de Castro, R. Treusch, L. Strüder, T. Möller, and C. Bostedt, Identification of twinned gas phase clusters by single-shot scattering with intense soft x-ray pulses, New J. Phys. **14**, 055016 (2012).
[57] H. Pauly, *Atom, Molecule, and Cluster Beams I*, 1st ed., Springer Series on Atomic, Optical, and Plasma Physics Vol. 28 (Springer Berlin Heidelberg, Berlin, Heidelberg, 2000), p. 334.
[58] M. Hartmann, R. E. Miller, J. P. Toennies, and A. Vilesov, Rotationally Resolved Spectroscopy of SF_6 in Liquid Helium Clusters: A Molecular Probe of Cluster Temperature, Phys. Rev. Lett. **75**, 1566 (1995).
[59] R. Jansen, N. Gimelshein, S. Gimelshein, and I. Wysong, A Lagrangian–Eulerian approach to modeling homogeneous condensation in high density gas expansions, J. Chem. Phys. **134**, 104105 (2011).
[60] O. F. Hagena, Cluster ion sources (invited), Rev. Sci. Instrum. **63**, 2374 (1992).
[61] F. Dorchies, F. Blasco, T. Caillaud, J. Stevefelt, C. Stenz, A. S. Boldarev, and V. A. Gasilov, Spatial distribution of cluster size and density in supersonic jets as targets for intense laser pulses, Phys. Rev. A **68**, 023201 (2003).
[62] G. I. Harris, D. L. McAuslan, E. Sheridan, Y. Sachkou, C. Baker, and W. P. Bowen, Laser cooling and control of excitations in superfluid helium, Nat. Phys. **12**, 788 (2016).
[63] K. K. Lehmann and A. M. Dokter, Evaporative Cooling of Helium Nanodroplets with Angular Momentum Conservation, Phys. Rev. Lett. **92**, 173401 (2004).
[64] R. E. Grisenti and J. P. Toennies, Cryogenic Microjet Source for Orthotropic Beams of Ultralarge Superfluid Helium Droplets, Phys. Rev. Lett. **90**, 234501 (2003).
[65] S. Kuma and T. Azuma, Pulsed beam of extremely large helium droplets, Cryogenics **88**, 78 (2017).
[66] D. Verma and A. F. Vilesov, Pulsed helium droplet beams, Chem. Phys. Lett. **694**, 129 (2018).
[67] P. Behrens, Charakterisierung von gepulsten Clusterquellen, Master's thesis, Technische Universität Berlin, 2019.
[68] R. M. P. Tanyag, A. J. Feinberg, S. M. O. O'Connell, and A. F. Vilesov, Disintegration of diminutive liquid helium jets in vacuum, J. Chem. Phys. **152**, 234306 (2020).
[69] R. M. P. Tanyag *et al.*, Sizes of pure and doped helium droplets from single shot x-ray imaging, J. Chem. Phys. **156**, 041102 (2022).
[70] J. Wörmer, M. Joppien, G. Zimmerer, and T. Möller, Formation and Confinement of Wannier Excitons in Free Argon Clusters, Phys. Rev. Lett. **67**, 2053 (1991).
[71] R. Karnbach, M. Joppien, J. Stapelfeldt, J. Wörmer, and T. Möller, CLULU: An experimental setup for luminescence measurements on van der Waals clusters with synchrotron radiation, Rev. Sci. Instrum. **64**, 2838 (1993).
[72] U. Even, Pulsed supersonic beams from high pressure source: Simulation, results, and experimental measurements, Adv. Chem. **2014**, 636042 (2014).
[73] M. D. Morse, 2—Supersonic beam sources, in *Atomic, Molecular, and Optical Physics: Atoms and Molecules*, Experimental Methods in the Physical Sciences Vol. 29, edited by F. Dunning and R. G. Hulet (Academic Press, New York, 1996), pp. 21–47.
[74] W. Christen, Stationary flow conditions in pulsed supersonic beams, J. Chem. Phys. **139**, 154202 (2013).
[75] M. N. Slipchenko, S. Kuma, T. Momose, and A. F. Vilesov, Intense pulsed helium droplet beams, Rev. Sci. Instrum. **73**, 3600 (2002).
[76] S. Yang, S. M. Brereton, and A. M. Ellis, Controlled growth of helium nanodroplets from a pulsed source, Rev. Sci. Instrum. **76**, 104102 (2005).
[77] D. Pentlehner, R. Riechers, B. Dick, A. Slenczka, U. Even, N. Lavie, R. Brown, and K. Luria, Rapidly pulsed helium droplet source, Rev. Sci. Instrum. **80**, 043302 (2009).
[78] R. Katzy, M. Singer, S. Izadnia, A. C. LaForge, and F. Stienkemeier, Doping He droplets by laser ablation with a pulsed supersonic jet source, Rev. Sci. Instrum. **87**, 013105 (2016).
[79] R. Pandey, S. Tran, J. Zhang, Y. Yao, and W. Kong, Bimodal velocity and size distributions of pulsed superfluid helium droplet beams, J. Chem. Phys. **154**, 134303 (2021).
[80] R. D. Mc Carty, Thermodynamic properties of helium 4 from 2 to 1500 K at pressures to 10^8 Pa, J. Phys. Chem. Ref. Data **2**, 923 (1973).
[81] R. A. Brown and L. E. Scriven, The shape and stability of rotating liquid drops, Proc. R. Soc. A **371**, 331 (1980).
[82] F. Ancilotto, M. Barranco, and M. Pi, Spinning superfluid ^{4}He nanodroplets, Phys. Rev. B **97**, 184515 (2018).

[83] M. Pi, J. M. Escartín, F. Ancilotto, and M. Barranco, Coexistence of vortex arrays and surface capillary waves in spinning prolate superfluid ^{4}He nanodroplets, Phys. Rev. B **104**, 094509 (2021).
[84] R. M. P. Tanyag, Imaging superfluid helium droplets, Ph.D thesis, University of Southern California, 2018.
[85] B. Langbehn *et al.*, Three-Dimensional Shapes of Spinning Helium Nanodroplets, Phys. Rev. Lett. **121**, 255301 (2018).
[86] S. W. Van Sciver and C. F. Barenghi, Chapter 5—Visualisation of Quantum Turbulence, in *Quantum Turbulence, Progress in Low Temperature Physics* Vol. 16, edited by M. Tsubota and W. Halperin (Elsevier, New York, 2009), pp. 247–303.
[87] G. H. Bauer, R. J. Donnelly, and W. F. Vinen, Vortex configurations in a freely rotating superfluid drop, J. Low Temp. Phys. **98**, 47 (1995).
[88] U. Giuriato, G. Krstulovic, and S. Nazarenko, How trapped particles interact with and sample superfluid vortex excitations, Phys. Rev. Res. **2**, 023149 (2020).
[89] M. S. Paoletti and D. P. Lathrop, Quantum turbulence, Annu. Rev. Condens. Matter Phys. **2**, 213 (2011).
[90] L. Madeira, M. Caracanhas, F. dos Santos, and V. Bagnato, Quantum turbulence in quantum gases, Annu. Rev. Condens. Matter Phys. **11**, 37 (2020).
[91] C. Raman, J. R. Abo-Shaeer, J. M. Vogels, K. Xu, and W. Ketterle, Vortex Nucleation in a Stirred Bose–Einstein Condensate, Phys. Rev. Lett. **87**, 210402 (2001).
[92] P. Rosenbusch, V. Bretin, and J. Dalibard, Dynamics of a Single Vortex Line in a Bose–Einstein Condensate, Phys. Rev. Lett. **89**, 200403 (2002).
[93] D. Rupp, N. Monserud, B. Langbehn, M. Sauppe, J. Zimmermann, Y. Ovcharenko, T. Möller, F. Frassetto, L. Poletto, A. Trabattoni, F. Calegari, M. Nisoli, K. Sander, C. Peltz, M. J. Vrakking, T. Fennel, and A. Rouzée, Coherent diffractive imaging of single helium nanodroplets with a high harmonic generation source, Nat. Commun. **8**, 493 (2017).
[94] G. M. Seidel and H. J. Maris, Morphology of superfluid drops with angular momentum, Physica (Amsterdam) **194-196B**, 577 (1994).
[95] L. Childress, M. P. Schmidt, A. D. Kashkanova, C. D. Brown, G. I. Harris, A. Aiello, F. Marquardt, and J. G. E. Harris, Cavity optomechanics in a levitated helium drop, Phys. Rev. A **96**, 063842 (2017).
[96] B. Langbehn *et al.*, Diffraction imaging of light induced dynamics in xenon-doped helium nanodroplets, New J. Phys. **24**, 113043 (2022).
[97] 10.22003/XFEL.EU-DATA-002195-00.